Materials Research Proceedings 41 (2024) 586-594 https://doi.org/10.21741/9781644903131-65

Transverse squeeze flow of fibre reinforced thermoplastic composites

BIELEMAN Gerben[1,2,a,*], ROTINK Gijs[1], GROUVE Wouter J.B.[1,2], KLOMPEN Edwin T.J.[2] and AKKERMAN Remko[1,2]

[1]Faculty of Engineering Technology, Chair of Production Technology, University of Twente, Enschede, the Netherlands

[2]ThermoPlastic composites Research Center (TPRC), Enschede, the Netherlands

[a]g.bieleman@utwente.nl

Keywords: Squeeze Flow, Transverse Viscosity, Thermoplastic Composites

Abstract. Transverse squeeze flow is one of the deformation mechanisms that govern the forming of molten fiber reinforced thermoplastic composites. It is typically described by a transverse bulk viscosity, dictating the resistance against the flow of the combined constituents. In this work, the squeeze flow method was used to characterize the transverse viscosity of carbon fiber reinforced low-melting PAEK at three different compression rates. The experiments were recorded with a camera and the video images were analyzed to obtain the flow fields. A power law fluid model was fitted to the logged data, but found to be unable to describe the material behavior at all compression rates. Moreover, the video analyses indicated discrepancies between the observed specimen deformations and those predicted by the model. Future studies need to focus on the description of the squeeze flow behavior of UD C/LM-PAEK by different models (viscous, viscoelastic), using video-captured deformations for numerical fitting of the models.

Introduction

In the last decade, thermoplastic composites (TPCs) have seen increased application in parts and structures for the automotive and aerospace industries. TPCs possess high specific mechanical properties and provide advantages in terms of automation and assembly compared to their thermoset counterparts [1]. Notably, the melt-processability of the thermoplastic matrix allows for short processing times, via for example press-forming, and for assembly by means of fusion bonding. The design of production and assembly processes for TPCs can be facilitated by predictive process design tools that allow for virtual tool and process optimizations [2] to achieve first-time-right manufacturing. These tools require an accurate description of the material behavior and deformation mechanisms during processing, including for example intraply shear, bending and friction [3,4,5]. Transverse squeeze flow is another deformation mechanism, that takes place during processing, especially in the case of a mismatch between tool cavity and blank thickness where it can lead to changes in the local microstructure, affecting the mechanical performance of the manufactured part. The inclusion of transverse squeeze flow in predictive simulation software requires reliable constitutive models and the associated characterization methods, which are not yet readily available. The literature describes a selection of methods with which the transverse flow behavior of unidirectional (UD) TPCs can be characterized [6]. This work will employ the so-called squeeze flow method[7,8] to characterize the transverse viscosity of UD C/LM-PAEK material.

Background

The squeeze flow method typically involves the compression of molten thermoplastic material between two heated compression platens. In this particular case, UD fiber reinforced TPC material will be considered. The experiments are conducted by compressing specimens at a fixed rate to a certain percentage of their original thickness whilst logging the required force and displacement,

Materials Research Proceedings 41 (2024) 586-594 https://doi.org/10.21741/9781644903131-65

schematically shown in Figure 1. The flow between the platens can take different velocity profiles based on the boundary conditions between the specimen and compression platen. These conditions are shown in Figure 2, with Figure 2a showing the so-called plug flow which occurs when there is full slip between the specimen and the compression platen and Figure 2b describing shear flow with zero slip at the boundary. Figure 2c describes a combined profile of plug flow and shear flow, which may occur when there is a stick-slip response at the boundary. Viscous or viscoelastic models can be fitted based on the logged force and displacement, taking into account the boundary conditions during the experiment.

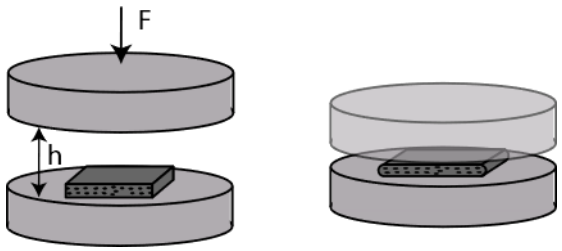

Figure 1: Squeeze flow experiment

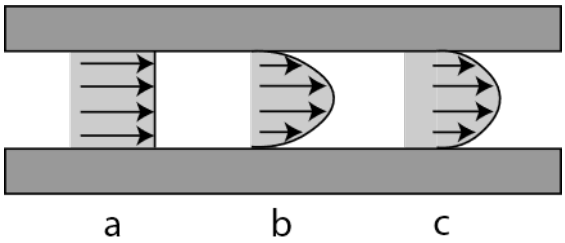

Figure 2: Flow types between parallel plates

Problem statement

Currently, the squeeze flow of high fiber-filled UD carbon fiber polyaryletherketones (C/PAEKs) cannot be characterized accurately. Slange indicates in his PhD thesis that the literature does not contain a suitable model for the transverse viscosity of C/PEEK in the temperature window of 340 °C to 400 °C [9]. Moreover, the literature review by Wang et al. shows a wide range of transverse viscosity values for high fiber-filled C/PAEKs [6], with differences in the characterization of C/PEEK up to an order of magnitude. Furthermore, these transverse viscosity characterizations were obtained with various methods. It can be concluded that there is no established methodology and model to describe the transverse squeeze flow of C/PAEK composites. Moreover, up to the author's best knowledge, the transverse squeeze flow behavior of carbon fiber low-melting polyaryletherketone (C/LM-PAEK) has not been characterized yet in the literature. This study aims to characterize the transverse viscosity of UD C/LM-PAEK composites using the squeeze flow method. A power law fluid model is used to fit the experimental data.

Material

The material used in this study was C/LM-PAEK TC1225, by Toray Advanced Composites [10]. The material was consolidated according to the manufacturer's specifications into UD laminates with a thickness of 64 plies (9.2 mm) on a Pinette press in a 12 by 12 in^2 picture frame mold. Specimens were milled from the UD laminates, with in-plane dimensions of 50 by 50 mm^2. Markings were applied to one of the sides with the exposed fiber ends, to visualize the deformation during testing, displayed in Figure 3. Lastly, 0.05mm thick M-Tech F metal foils by Martin [11], were cut to 150 by 75 mm^2, cleaned with IPA, and placed above and underneath the specimens during the experiments for sample removal between measurements.

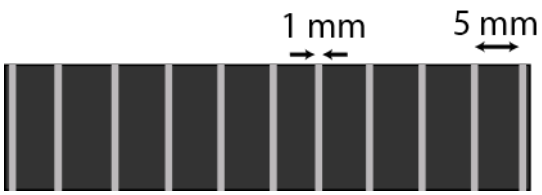

Figure 3: Markings for visualization of the flow front of squeeze flow specimens

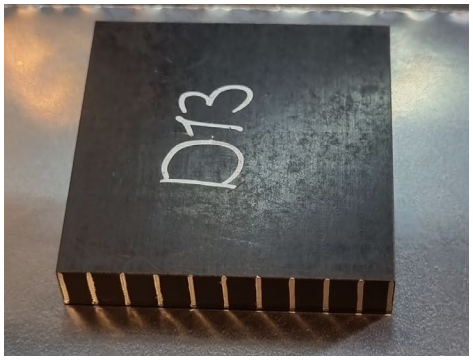

Figure 3: Specimen before squeeze flow experiment

Methodology

Squeeze flow tests were performed by compressing the specimens between two heated compression plates while logging force and displacement. The experiments were performed on a compression paten fixture, which was mounted in an INSTRON universal testing machine, shown in Figure 5. The setup contains two heated and temperature-controlled compression platens. Furthermore, the setup makes use of two linear variable differential sensors (LVDT) to measure the relative displacement between both compression platens.

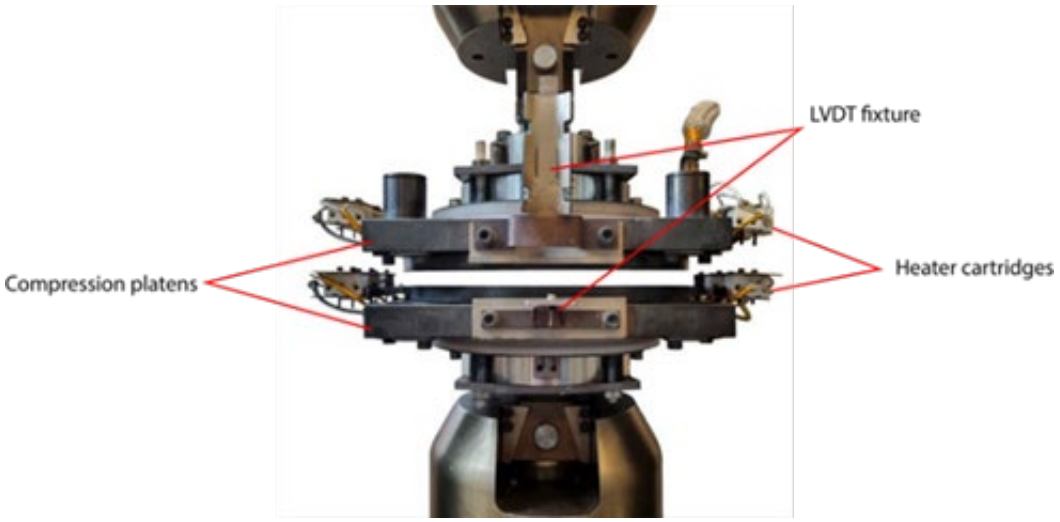

Figure 4: Experimental setup for squeeze flow characterization

All squeeze flow experiments were carried out according to the same experimental procedure. The specimens were first taken out of a vacuum oven where they were stored after manufacturing to ensure that they were dry. The specimens were placed between two metal foils in the center of the bottom compression fixture. The metal foils facilitate specimen removal and assure a no-slip boundary condition between the specimens, which was verified by video analyses of the markings on the specimens. The top compression platen was placed 3 mm above the specimen. Subsequently, the specimen was heated to a temperature of 360°C in 7 minutes ensuring a uniform temperature throughout the specimen. The experimental procedure was started by moving the top compression fixture downwards until a force of 20 N was registered, after which the set compression rate in the form of a constant displacement rate of the top compression platen was prescribed. Three displacement rates were considered, namely 0.01, 0.1 and 1.0 mm/s. The experiment consists of compressing the specimen down to 40% of the original thickness (60%

compression ratio). All experiments were performed in triplets, using a new specimen for each test.

An analytical plane strain model for incompressible creeping shear flow with a no-slip condition at the wall was used to describe the transverse squeeze flow of the C/LM-PAEK samples for this experimental setup [12]. The flow was assumed to take place transverse to the fiber direction. In this model, the bulk viscosity of the molten TPC was described as a power law fluid, with a viscosity parameter *k* and a shear rate dependence parameter *n*. The model provides an equation for the compression force *Fc*, described by Equation 1.

$$\boldsymbol{F_c = \left(\frac{\dot{h}^n}{h^{2n+1}}\right)\left(\frac{2n+1}{n}\right)^n\left(\frac{k_s L w^{(n+2)}}{n+2}\right)} \quad (1)$$

in which $\dot{h}$ describes the compression rate, *h* de current specimen thickness, *L* the length of the specimen in fiber direction and *w* the current width of the specimen. The width of the specimen *w* was calculated based on the assumption of constant volume.

The deformation of the specimens during the experiments was captured in real time using a camera mounted on a tripod stand. The velocity field was extracted from the footage with the use of MATLAB code by tracking the marked lines. So-called regions of interest were manually selected in the video file on one of the lines, as shown in Figure 6. Around these selected regions of interest, boxes were drawn in which points with steep greyscale gradients were selected [13]. These points were tracked throughout the video by means of a KLT algorithm [14,15]. The location of the tracked points was marked and stored. The stored locations, combined with the time between frames, were used to determine the velocity of these points. A comparison between the obtained velocity in the points and the velocity profile assumed by the analytical fitted power law fluid model could be made, to give insight into the models' accuracy. The velocity assumed by the fitted power law model can be described by Equation 2.

$$V_x(x,z) = -\dot{h}\left(\frac{1+2*n}{1+n}\right)\left(\frac{1}{h}\right)^{\frac{1+2n}{n}} 2^{\left(\frac{1}{n}+1\right)} x\left[z^{\frac{1}{n}+1} - \left(\left(\frac{h}{2}\right)^{\frac{1}{n}+1}\right)\right] \quad (2)$$

Figure 5: Points traced (yellow stars) on a line to obtain the local velocity during the squeeze flow of a specimen

Results

The averaged results of the force versus the compression ratio for the three different compression rates are shown by the solid lines in Figure 7. The results show a start-up phase between 0% and 15% compression. The plot shows that an increase in compression rate yields an increase in force response. The data across the three measured samples per compression rate is depicted by the colored areas around the solid lines and shows little deviation between measurements. The fitted power law fluid model is shown by the dashed lines. The data was fitted between the compression range of 15% to 30% and was extrapolated across the full plotted compression range. The model was fitted to the measured data for all compression rates, obtaining fitting parameters *k* =1.89e4 Pas and *n* =0.663.

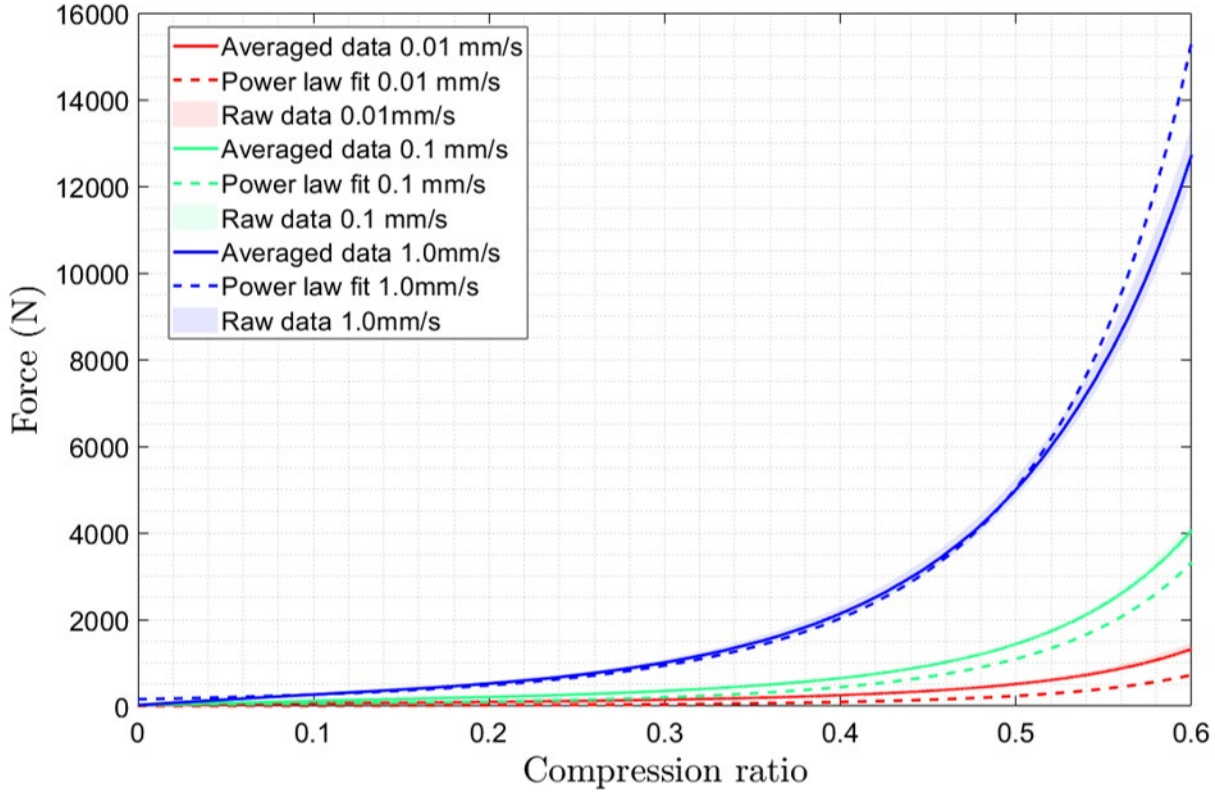

Figure 6: Force versus compression ratio of raw squeeze flow data, averaged data and fitted model

The velocity of the line with the yellow stars in Figure 6 was analyzed for the three different compression rates and evaluated at 15% and 30% compression. Figure 8a shows the velocity in the tracked points on the line in Figure 6 (circles) at a compression of 15%, as well as the line which describes the velocity assumed by the fitted power law model. Figure 8b shows the zoomed-in plot of Figure 8a, to clearly show the results at the lower compression rates. Similarly, Figures 8c and 8d show the velocity profile of the line at 30% compression.

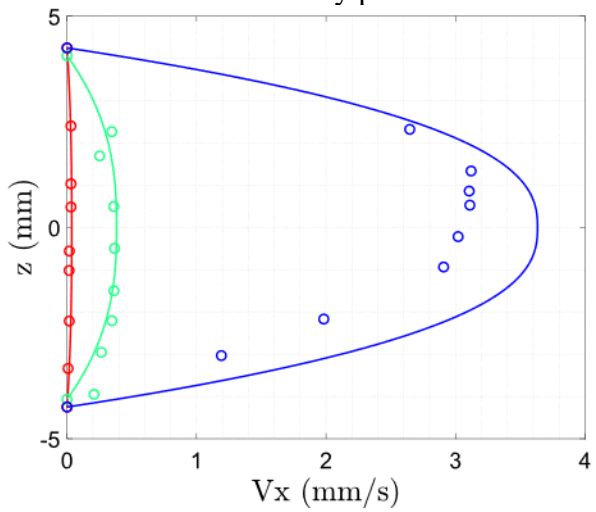

(a) Velocity profiles 15% compression

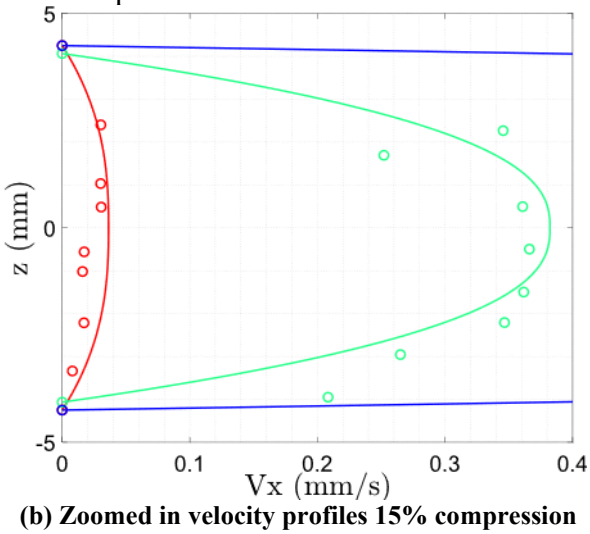

(b) Zoomed in velocity profiles 15% compression

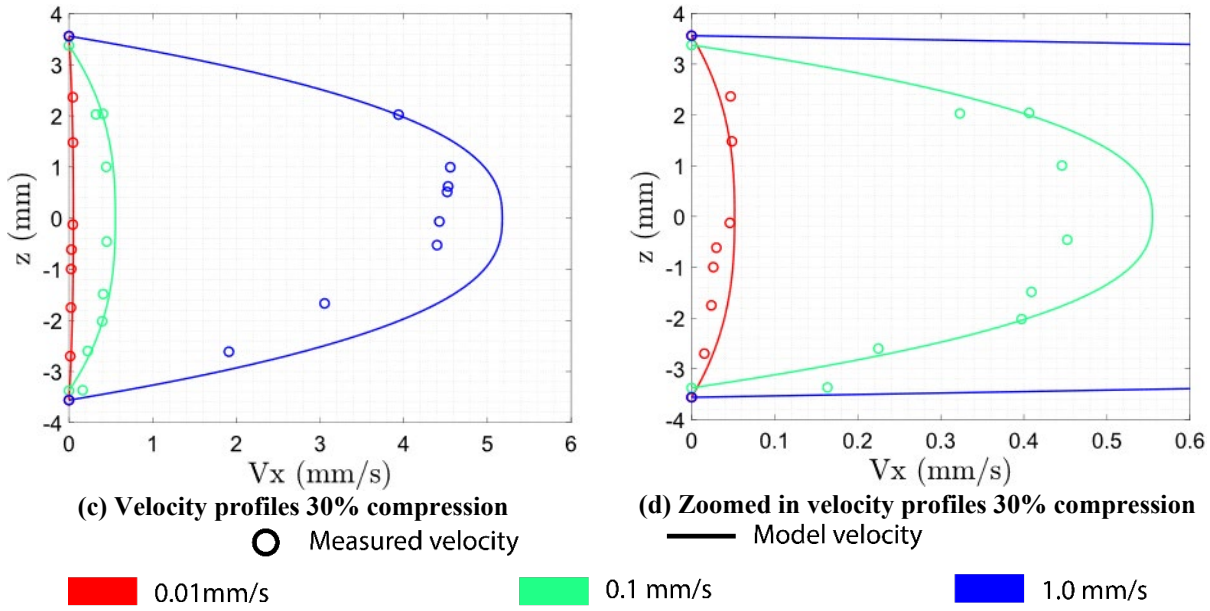

Figure 7: Velocity profiles of the tracked line from Figure 6

Discussion

Start-up effects. The start-up effects shown in Figure 7 take place between 0% to 15% compression. These effects were excluded when fitting the power law fluid model. However, this start-up phase contains useful information, as in practical applications squeeze flow mostly takes place in scenarios with limited deformation. Henceforth, to describe press-forming or fusion bonding processes there is the need to understand what the contributions to the start-up phase are. Rasheed mentioned in his PhD thesis that this start-up phase contains the development of the shear flow front at the edges of the specimen, a condition assumed for the power law fluid model [12]. Further observations from the video footage show the deconsolidation of the specimens during heating of the specimens. The specimens rapidly increase in thickness during heating and start to form cracks as shown in Figure 9, with a specimen before heating on the left and the deconsolidated specimen on the right after heating. The cause of deconsolidation is likely due to elastic stresses stored in the fiber bed during manufacturing [16]. The effects of moisture could be excluded, as the specimens were stored in a vacuum oven. The cracks were observed to be partially reconsolidated during the initial compression phase. Given the observed deconsolidation, it is likely that part of the start-up response is due to reconsolidation.

Figure 8: Deconsolidation of a specimen during heating, left image before heating, right image after heating with deconsolidation (cracks) at the red arrows

Boundary condition changes. The fitting of the power law fluid model could only be performed up to 30% compression, due to changes occurring in the fluid velocity field. The model used the assumption of shear flow within the specimen. However, at 30% compression, the flow field starts to change near the edges of the specimen from a shear flow profile to a so-called fountain flow profile. Figure 10 shows a micrograph of the edge of one of the specimens. The red arrows indicate the fountain flow originating from the center of the specimen and flowing towards the top and bottom surfaces. Figure 11 shows the onset of this fountain flow on the right side of the specimen

where the outer edges start to split up from the center. In some of the footage taken during the squeeze flow experiments, this splitting near the center of the specimen's edge seemed to originate from pre-existing cracks that formed during the heating as a result of deconsolidation.

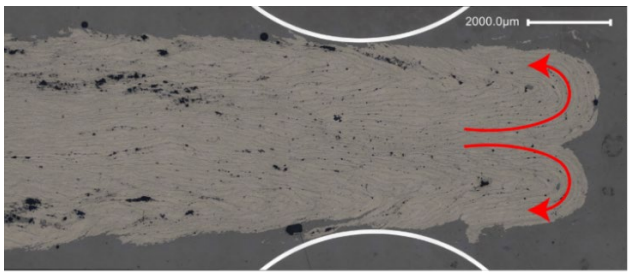

Figure 9: Fountain flow, indicated with red arrows from the center of the sample to top and bottom surface

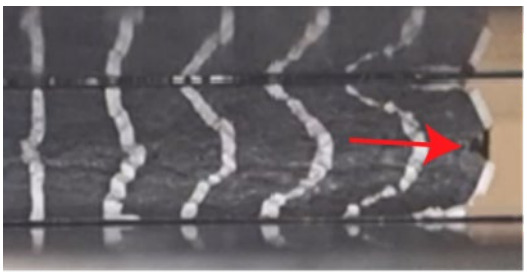

Figure 10: Onset of fountain flow resulting from a crack at the specimen edge (red arrow)

Power law fluid model. The power law fluid model fit displayed in Figure 7 shows an inability to describe the squeeze flow behavior of C/LM-PAEK. There are discrepancies between the model and measured force versus compression ratio at all compressoin rates. There could be a few causes for this inability to describe the squeeze flow of C/LM-PAEK. The first could be the type of fluid model selected. The choice for a power law fluid was made as it can be analytically fitted to the data. The material may show different viscous behavior, Moreover, it is well established that a polymer melt exhibits viscoelastic material behavior. Lastly, the assumption was made that no interactions between the solid fibers of the TPC melt would contribute to the deformation behavior during the squeeze. This assumption could be an oversimplification and possibly needs further exploration.

Velocity profiles. The velocity profile of the fitted power law fluid model and the measured velocity in the tracked points in Figure 8 show discrepancies, with the velocity assumed by the model overpredicting the observed values. In some instances, this overprediction was only a negligible amount, such as the velocity for the compression rate of 0.1 mm/s (green) in Figure 8b. However, in most cases, the velocity is significantly overpredicted by the model, up to as much as 30%. Moreover, the shape of the solid lines may differ from that of the imaginary line drawn through the measured points. The shape of the fitted line is based on the power law fluid model with the fitted parameter *n.* As stated earlier, the power law fluid model was not able to describe the flow behavior and will therefore also inaccurately describe the velocity field in the sample. In addition, the local differences in observed velocity field could be partly due to localized effects which seem to be the result of local slip between plies occurring during compression. This slip between plies is shown in Figure 11, yielding the jagged-like parabolic lines. It has to be noted that the validity of these results is limited to one of the single lines on the specimen, for better insight into the deformation of the specimen all lines need to be traced. Furthermore, lines are not ideal for the video tracking of a velocity in a single point. The identification of the regions of interest around these lines only has a grayscale gradient in one direction, where preferably it should be in both in-plane directions. The accuracy of the tracked points in z-direction was deemed limited, due to the previously mentioned reason. A grid of points would be a better choice to capture the specimens' deformations under squeeze flow conditions as a point possesses a greyscale gradient in both directions. More accurate measurements of the velocity field could in turn aid in the numerical fitting of different viscous or viscoelastic models to the squeeze flow response of UD C/LM-PAEK.

Summary
This work aimed to characterize the transverse squeeze flow of UD C/PAEK composites, based on the squeeze flow characterization methodology. To this extent, squeeze flow experiments were performed at three compression rates to obtain the force versus compression ratio response of UD C/LM-PAEK specimens. An analytical power law fluid model with a transverse bulk viscosity was fitted to the data. The implemented model was not able to describe the material behavior of C/LM-PAEK for the experimental conditions. Analysis of the flow, by means of the velocity of a marking on the specimens' side showed discrepancies between the velocity obtained from the video images and the velocity based on the fitted power law model. Future research should focus on the description of the squeeze flow of C/PAEK, by means of a different viscous or viscoelastic model, with numerical fitting based on the captured specimen deformation during the squeeze flow experiments.

Acknowledgments
This work was performed as part of the Perspectief research program Enlighten, which is financed by the Dutch Research Council (NWO). The authors also gratefully acknowledge the in-kind and technical support from the industrial and academic members of the ThermoPlastic composites Research Center (TPRC)

References

[1] A.R. Offringa, "Thermoplastic composites - Rapid processing applications," Composites Part A: Applied Science and Manufacturing, vol. 27, no. 4 PART A, pp. 329–336, 1996.

[2] A.C. Long, Composites forming technologies. Elsevier. 2014

[3] U. Sachs, Friction and bending in thermoplasctic composites forming processes p. 101 . 2014. Enschede, Netherlands,: University of Twente.

[4] D. Brands, L.G. di Genova, E.R. Pierik, W.J.B. Grouve, S. Wijskamp, R. Akkerman, Formability experiments for unidirectional thermoplastics composites, in: 25th International Conference on Material Forming, Braga, Portugal: ESAFORM, 2022, pp. 1358-1371

[5] J.S.U. Schell, J. Guilleminot, C. Binetruy, and P. Krawczak, "Computational and experimental analysis of fusion bonding in thermoplastic composites: Influence of process parameters," Journal of Materials Processing Technology, vol. 209, no. 11, pp. 5211–5219, Jun. 2009, doi: https://doi.org/10.1016/j.jmatprotec.2009.03.008

[6] J. Wang et al., "A review of experimental methods for characterising composite viscosities of continuous fibre-reinforced polymer composites," Korea-australia Rheology Journal, vol. 35, no. 2, pp. 57–68, Feb. 2023, doi: https://doi.org/10.1007/s13367-023-00053-2

[7] S.F. Shuler and S.G. Advani, "Transverse squeeze flow of concentrated aligned fibers in viscous fluids," Journal of Non-Newtonian Fluid Mechanics, vol. 65, no. 1, pp. 47–74, Jul. 1996, doi: https://doi.org/10.1016/0377-0257(96)01440-1

[8] T.G. Rogers, "Squeezing flow of fibre-reinforced viscous fluids," Journal of Engineering Mathematics, vol. 23, no. 1, pp. 81–89, Mar. 1989, doi: https://doi.org/10.1007/bf00058434

[9] T.K. Slange, "Rapid Manufacturing of Tailored Thermoplastic Composites by Automated Lay-up and Stamp Forming: A Study on the Consolidation Mechanisms," research.utwente.nl, Mar. 2019, doi: https://doi.org/10.3990/1.9789036547284

[10] "Toray Cetex® TC1225 - Toray Advanced Composites," Advanced Composites. https://www.toraytac.com/product-explorer/products/gXuK/Toray-Cetex-TC1225

[11] “Liefersortiment M-Tech ® F -Metallfolienbänder,” 2011. https://georgmartin.com/wp-content/uploads/2022/02/Liefersortiment_M-Tech-F_Boxen.pdf

[12] M. Iqbal, “Compression molding of chopped woven thermoplastic composite flakes: a study on processing and performance,” May 2016, doi: https://doi.org/10.3990/1.9789036541510

[13] L.D. Bruce and T. Kanade. “An Iterative Image Registration Technique with an Application to Stereo Vision,”Proceedings of the 7th International Joint Conference on Artificial Intelligence, April, 1981, pp. 674–679.

[14] J. Shi and C. Tomasi, "Good Features to Track," Proceedings of the IEEE Conference on Computer Vision and Pattern Recognition, June 1994, pp. 593–600.

[15] C. Tomasi and T. Kanade, Detection and Tracking of Point Features, Computer Science Department, Carnegie Mellon University, April, 1991.

[16] L. Amedewovo, L. Orgéas, B. de Parscau du Plessix, N. Lefèvre, A. Lévy, and S. Le Corre, “Deconsolidation of carbon fiber-reinforced PEKK laminates: 3D real-time in situ observation with synchrotron X-ray microtomography,” Composites Part A: Applied Science and Manufacturing, vol. 177, pp. 107917–107917, Feb. 2024, doi: https://doi.org/10.1016/j.compositesa.2023.107917